Clays and Clay Minerals, Vol. 49, No. 4, 333–346, 2001.

DIAGENESIS OF DIOCTAHEDRAL AND TRIOCTAHEDRAL SMECTITES FROM ALTERNATING BEDS IN MIOCENE TO PLEISTOCENE ROCKS OF THE NIIGATA BASIN, JAPAN

BYEONG-KOOK SON[1], TAKAHISA YOSHIMURA[2,*] AND HIKARU FUKASAWA[3]

[1] Korea Institute of Geoscience and Mineral Resources (KIGAM), 30, Kajungdong, Yusungku, Taejon, Korea
[2] Department of Environmental Sciences, Faculty of Sciences, Niigata University, Ikarashi-2, Niigata, Japan
[3] Exploration Department, Japan Petroleum Exploration Co. Ltd, Higashi-Shinagawa, Tokyo, Japan

Abstract—Clay mineral diagenesis in the Niigata basin is documented by mineralogical and chemical analysis of clay minerals from cuttings from the Shinkumoide SK-1D (SSK-1D) well which is characterized by alternating beds containing dioctahedral and trioctahedral smectite minerals with increasing depth. Dioctahedral smectite shows a progressive increase in illite interstratification with increasing depth. The transition of dioctahedral smectite to interstratified illite-smectite (I-S) is supported chemically by an increase in K and Al and a decrease in Si with increasing depth. In contrast, trioctahedral smectite (saponite) reacts to form a 1:1 interstratified chlorite-smectite (C-S) with increasing burial depth and temperature. Considering the geology and the occurrence of smectite, the SSK-1D smectites probably altered diagenetically from two different parent materials: dioctahedral smectite is derived from clastic sediments and transforms to interstratified illite-smectite, whereas trioctahedral smectite is derived from andesitic pyroclastic rocks and transforms to interstratified chlorite-smectite.

The C-S occurs at the same depth of ~3200 m as the conversion of randomly interstratified (R = 0) I-S to (R = 1) I-S. Furthermore, the depth is compatible with a T_{max} temperature of 430–435°C, which indicates the starting temperature for oil generation from organic matter. The temperature of the conversion of (R = 0) I-S to (R = 1) I-S and the start of corrensite formation is estimated at 110–120°C based on the time-temperature model suggested by others. The clay-mineral diagenesis in the SSK-1D further suggests that I-S and C-S can act as geothermometers in clastic and pyroclastic sediments provided that the effect of time is considered.

Key Words—Chlorite-Smectite, Clay Mineral Diagenesis, C-S, Geothermometer, Illite-Smectite, I-S, Niigata Basin, Saponite.

INTRODUCTION

The progressive transformation of smectite is volumetrically the most important diagenetic clay reaction during the progressive burial of sedimentary sequences; dioctahedral smectite transforms into illite via interstratified illite-smectite (I-S), and trioctahedral smectite transforms into chlorite via interstratified chlorite-smectite (C-S). The transformation of dioctahedral smectite to illite is widely recognized in fine-grained clastic sediments throughout the world (Perry and Hower, 1972; Hower *et al.*, 1976; Son and Yoshimura, 1997). The reaction of dioctahedral smectite to illite is a continuous series of I-S; the proportion of illite layers in I-S increases with depth in response to increasing temperature or time. The mechanism of the smectite-to-illite reaction has been examined over the past few decades (Nadeau *et al.*, 1984; Altaner and Ylagan, 1997). In addition, the study of I-S diagenesis has been stimulated partly by an economic interest in finding more efficient methods to prospect for petroleum. Therefore, clay mineral diagenesis has been applied to petroleum exploration as a geothermometer to constrain the thermal history of basins to predict source-rock maturation better (Eslinger and Pevear, 1988; Pytte and Reynolds, 1989; Elliott *et al.*, 1991). The change of trioctahedral smectite to chlorite is dominant in sediments associated with mafic volcanic or evaporitic rocks (Yoshimura, 1983; Chang *et al.*, 1986; Inoue and Utada, 1991; Hillier, 1993). In contrast to I-S with changes in layer proportions, the reaction involving trioctahedral smectite has been considered as a prograde sequence of three phases: smectite, corrensite (1:1 C-S) and chlorite (Shau *et al.*, 1990; Inoue and Utada, 1991; Beaufort *et al.*, 1997). Thus, corrensite, the intermediate part of the sequence, is a discrete phase, rather than an interstratification of smectite and chlorite layers. The number of studies of the trioctahedral smectite-to-chlorite transformation is limited compared to those devoted to the transformation of dioctahedral smectite to illite, probably because C-S is restricted to mafic associations of volcaniclastics or evaporites.

In the Japanese islands, I-S and C-S transformations have primarily been investigated as they relate to hydrothermal alteration (Inoue and Utada, 1983; Inoue, 1987; Inoue *et al.*, 1987). However, several thick sedimentary sequences where the transition of smectite to illite or to chlorite probably occurs are present in Ter-

* Present address: 7910-22, 2-No-Cho, Ikarashi, Niigata, Japan.

Figure 1. Location of the Shinkumoide SK-1D well, and the distribution of marine sediments for each formation in the Niigata basin (modified from Sato *et al.*, 1995). A deep section of turbidite facies is developed to the west of the dotted line. However, mudstone facies are dominant to the north and east of the line. Note that the Shinkumoide SK-1D well is located in the mudstone facies. LT—Lower Teradomari Formation; UT—Upper Teradomari Formation; SY—Shiiya Formation; NY—Nishiyama Formation.

tiary sediments. In these sedimentary basins, many drill holes have been made for hydrocarbon exploration and development. Recently, detailed studies of I-S were made in the Tertiary sedimentary basin where fine-grained sediments dominate (Son and Yoshimura, 1997; Niu *et al.*, 2000). These studies indicated I-S diagenesis and showed a typical profile of smectite similar to the Gulf Coast sediments (Hower *et al.*, 1976). In this profile from Japan, we show that both dioctahedral and trioctahedral smectites occur in the same well.

The purpose of the present study is to document clay mineral diagenesis observed in the Shinkumoide SK-1D (SSK-1D) exploration well which samples > 4000 m of sediments ranging in age from Miocene to Pleistocene, in the Niigata sedimentary basin (Figure 1). The well is dominated by fine-grained rocks including clastics and pyroclastics, and presents an ideal setting for clay mineral studies. This paper shows that the SSK-1D well displays both C-S and I-S reactions with increasing burial depth. In addition, the clay mineral changes are correlated with organic maturity data to calibrate temperatures in the well.

GEOLOGICAL SETTING

The Niigata sedimentary basin is a very thick marine sequence of clastic and pyroclastic sediments which accumulated during Miocene to Pleistocene. The basin was initially formed by the effect of rifting related to tensional back-arc spreading in Miocene time (Kobayashi and Yoshimura, 2000). In the Late Pliocene to Pleistocene, East–West compression resulted in many North–South trending folds and faults in the basin. This movement produced uplift and erosion in the southwestern and northern parts of the basin whereas, because of subsidence in the middle area of the basin, sedimentation continued after the Pliocene. Subsequently, the northern region subsided and was filled with fine-grained sediments. Lithologically, turbiditic sandstone predominates in the southern and western parts of the Niigata basin, whereas mudstones prevail in the middle and northern regions (Figure 1).

The SSK-1D well is located in the middle of the basin, geographically west of Nagaoka City, Niigata Prefecture (Figure 1). The well is located within the region characterized mainly by mudstone sediments, and penetrates a sedimentary succession of 4820 m of Miocene to Pleiostocene strata in the Niigata sedimentary basin. The sequences are divided into six formations: Lower Teradomari, Upper Teradomari, Shiiya, Nishiyama, Haizume and Uonuma Formations, in ascending order (Figure 2). The sequence of these formations is little disturbed by tectonic movement, ex-

https://doi.org/10.1346/CCMN.2001.0490407 Published online by Cambridge University Press

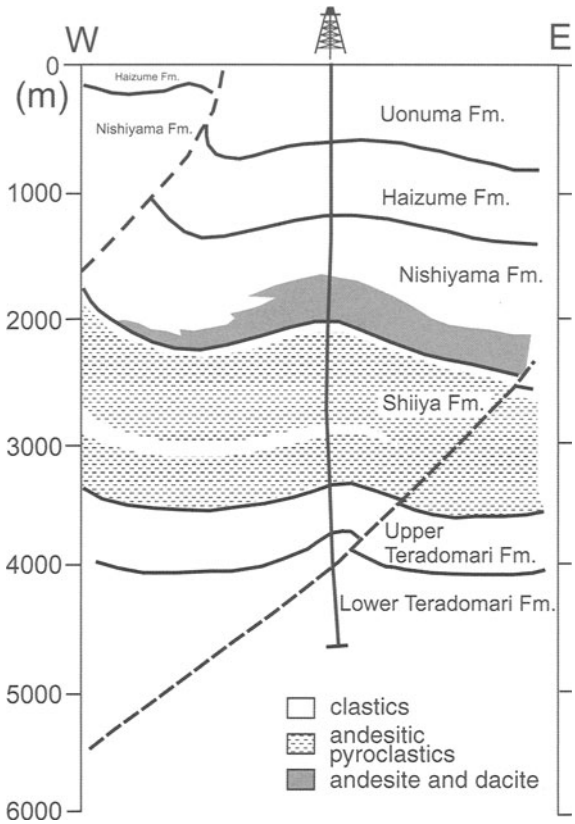

Figure 2. Diagrammatic cross-section of study area.

cept for gentle folds and faults in the Middle Pleistocene. The Lower and Upper Teradomari Formations consist primarily of clay-rich mudstones with occasional intercalation of tuff and sandstone. The deposition of the Teradomari Formation started at 14–13 Ma in a bathyal environment (Figure 3). During the Teradomari stage, a submarine fan developed in the southern part of the Niigata basin, while siliceous mudstone accumulated in the region including the SSK-1D well (Figure 1). The Shiiya Formation conformably overlies the Teradomari Formation and is composed predominantly of andesitic pyroclastic rocks, also deposited in the bathyal environment at 7 Ma. During the Shiiya stage, the SSK-1D was also dominated by a deposit of gray fine-grained clastic and volcaniclastic mudstones which accumulated at a greater rate of sedimentation than other formations. The Nishiyama Formation, overlying the Shiiya Formation, is composed mainly of fine mudstone with sandstone. The Nishiyama Formation includes dacite or andesite. Deposition of the Nishiyama Formation started at 4 Ma and in the SSK-1D is dominated by massive mudstone and sandy mudstone sequences. The Haizume and Uonuma Formations are also dominated by mudstones. Structurally, the formations at the SSK-1D well were folded gently and faulted by East–West compression during the Middle Pleistocene (Kobayashi *et al.*, 1991). The SSK-1D as a whole is a bathyal sequence of fine mudstones, and thus an ideal well for the study of clay mineral diagenesis.

MATERIALS AND METHODS

Cuttings were sampled at intervals of 200 m throughout the well and were then hand-picked to ensure representative lithology at different depths. Quantitative analyses of whole-rock samples were obtained by powder X-ray diffraction (XRD) and using the computer program SIROQUANT (Sietronics, 1996). This program is designed for the quantitative analysis of mineral phases based on the Rietveld technique. Chemical analyses of the whole-rock samples were performed by X-ray fluorescence (XRF) spectrometry on fused glass beads.

Cuttings were ground gently in distilled water, and dispersed in an ultrasonic bath. The suspension was centrifuged to obtain the following size-fractions: >2 μm, <2 μm and <0.2 μm. Following a filter transfer procedure (Moore and Reynolds, 1989), clay specimens of preferred orientation of the <2 μm fractions were prepared for XRD. Oriented specimens of the <0.2 μm fractions were also prepared by pipetting the suspensions onto a glass slide. The <2 and <0.2 μm specimens were air dried, saturated with ethylene glycol, and heated at 550°C, before analysis. Profiles were generated using a Rigaku RINT 1200 diffractometer with Ni-filtered CuKα radiation at 40 kV and 20 mA. The ratio of illite and smectite in I-S was determined by comparing the patterns obtained to tracings calculated using NEWMOD (Reynolds, 1985). Detrital clay minerals interfere with the determination of the I-S ratio, thus the <0.2 μm fractions were used in the analysis to minimize contamination and interference from coarser clays, *e.g.* illite, chlorite and kaolinite. The octahedral character of each clay mineral was determined from the position of the 060 reflection on XRD (random mounts, <2 μm fractions) and from chemical analysis.

Electron microprobe analyses were also performed on selected <0.2 μm clay powder samples that were prepared using the method of Son and Yoshimura (1997). Eight samples were selected for electron microprobe analysis: five of dioctahedral clays and three of the trioctahedral smectite (saponite), which include little or no clay mineral impurities except for kaolinite. To calculate the chemical formula of smectite and I-S, the amount of contaminating kaolinite, as determined by the quantitative analysis of the XRD patterns, was subtracted from the electron microprobe data.

Rock-Eval pyrolysis was performed on cuttings to obtain organic maturity data. About 100 mg of each sample was heated to 600°C in a Rock-Eval instrument (Espitalié *et al.*, 1985).

https://doi.org/10.1346/CCMN.2001.0490407 Published online by Cambridge University Press

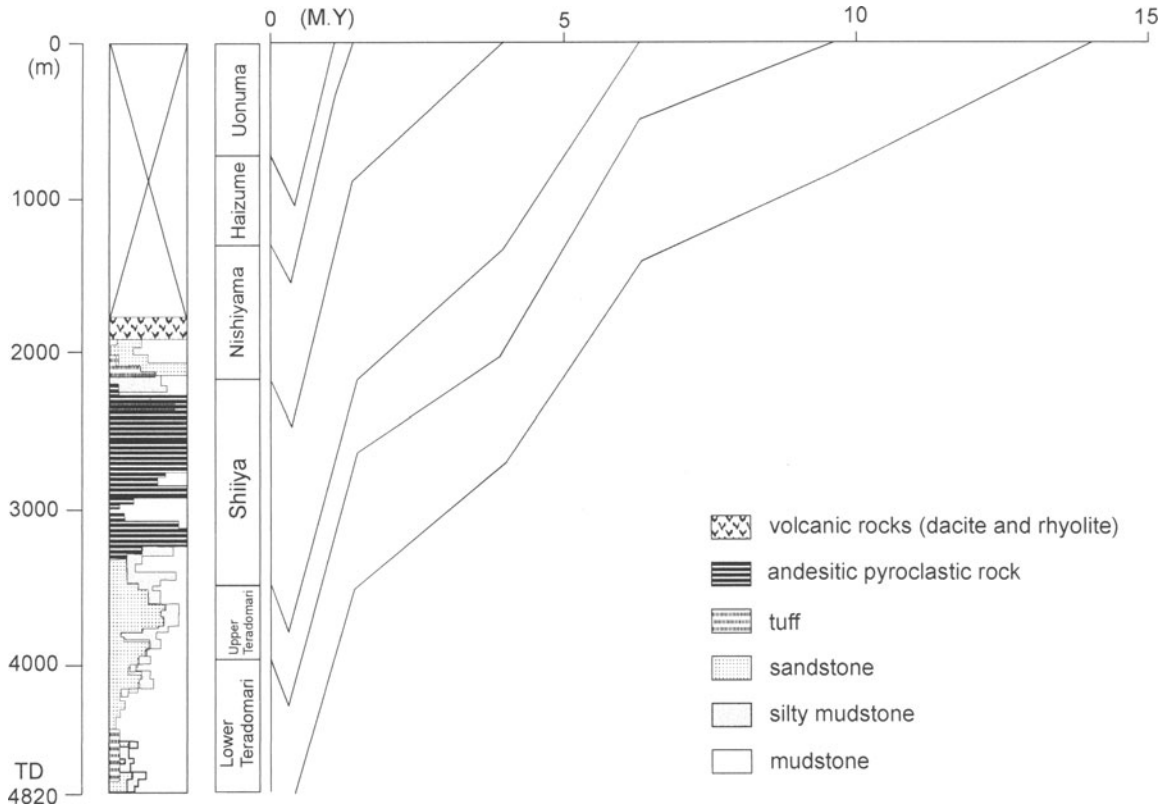

Figure 3. Stratigraphy, lithology and burial history of the Shinkumoide SK-1D well.

Table 1. Mineral composition of cuttings from the Shinkumoide SK-1D well.

Depth (m)	wt. % of mineral					
	Quartz	Plagioclase	K-rich feldspar	Zeolite	Amphibole	Clays (+ micas)
1200	28.2	20.6	8.2	—	—	43.0
1400	25.0	17.2	8.8	3.6	—	45.4
1600	26.8	18.4	9.2	1.8	—	43.8
1800	27.6	18.6	11.5	—	—	41.3
2000	30.5	21.9	7.4	—	—	40.2
2200	30.5	21.1	8.5	—	—	39.9
2400	6.8	55.9	15.3	—	—	22.0
2600	28.2	30.0	12.0	—	4.7	25.1
2800	33.1	21.9	14.0	—	—	31.0
3000	34.9	19.6	8.4	—	—	37.1
3200	25.8	36.5	10.4	—	—	27.3
3400	33.1	23.4	11.3	—	—	32.2
3600	36.1	26.5	6.6	—	—	30.8
3800	37.5	14.0	7.9	—	—	40.6
4000	35.0	20.2	10.1	—	—	34.7
4200	41.5	17.4	5.0	—	—	36.1
4400	35.6	21.5	4.2	—	—	38.7
4600	36.3	19.8	2.6	—	—	41.3
4800	40.5	16.4	2.2	—	—	40.9
4820	39.0	15.8	3.3	—	—	41.9

RESULTS

Whole-rock mineralogy and chemistry

X-ray diffraction shows that the mudstones primarily consist of clay minerals and fine-grained quartz and feldspar (mainly plagioclase) (Table 1, Figure 4). The mudstones also include zeolite (clinoptilolite) at shallow depths and amphibole at a depth of 2600 m. There is a variation in mineral abundance with increasing depth; quartz tends to increase with depth, whereas K-rich feldspar decreases. In comparison, plagioclase shows a distinct increase in abundance in intervals of andesitic pyroclastic rocks.

The chemical compositions of selected mudstones are shown in Table 2. The SiO_2 content in mudstone increases with depth, probably related to the increase in quartz. The MgO content is greater in the intervals between 2000–4000 m than at deeper and shallower levels. This variation can be attributed to andesitic pyroclastic rock present at 2000–4000 m.

Mineralogy of interstratified illite-smectite

Clay samples are characterized by high illite and kaolinite contents, thereby making the quantitative estimation of interstratified clay-mineral composition difficult. The <2 μm clay fractions are significantly contaminated by detrital minerals such as quartz and

https://doi.org/10.1346/CCMN.2001.0490407 Published online by Cambridge University Press

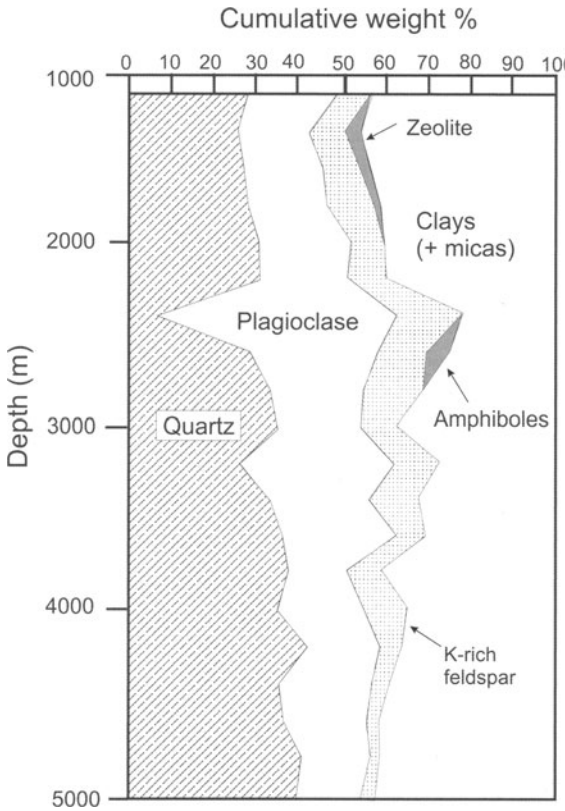

Figure 4. Change in whole-rock mineralogy with depth.

Table 2. Chemical analyses of cuttings from the Shinkumoide SK-1D well.

	1600 m	1800 m	2200 m	3200 m	3000 m
SiO_2	61.22	63.18	61.53	62.09	61.79
Al_2O_3	15.96	15.66	15.71	15.54	15.41
Fe_2O_3[1]	5.87	4.91	6.27	5.24	6.72
CaO	1.68	1.49	1.41	3.27	2.22
MgO	2.00	1.95	2.69	2.53	3.11
K_2O	3.13	3.24	2.84	2.74	2.83
Na_2O	2.37	2.51	2.43	3.02	2.32
TiO_2	0.70	0.64	0.68	0.52	0.65
MnO	0.05	0.05	0.06	0.08	0.08
P_2O_5	0.15	0.11	0.11	0.13	0.12
LOI[2]	6.75	6.00	6.05	4.47	4.47
Total	99.88	99.74	99.78	99.63	99.72
	3600 m	4000 m	4200 m	4600 m	4820 m
SiO_2	63.00	64.34	65.25	64.16	64.29
Al_2O_3	15.25	15.35	14.73	15.64	15.81
Fe_2O_3[1]	6.99	6.05	5.84	6.19	6.07
CaO	1.23	1.20	1.34	0.80	0.85
MgO	2.64	2.20	1.99	1.96	2.02
K_2O	3.02	3.13	2.80	2.97	2.94
Na_2O	2.08	2.01	2.07	2.23	2.16
TiO_2	0.66	0.64	0.62	0.64	0.61
MnO	0.05	0.05	0.06	0.06	0.05
P_2O_5	0.09	0.08	0.08	0.08	0.08
LOI[2]	4.79	4.74	4.96	5.08	4.94
Total	99.80	99.79	99.74	99.81	99.82

[1] Total Fe as Fe_2O_3.
[2] LOI: loss on ignition.

discrete illite. In comparison, the <0.2 μm fractions are nearly monomineralic, thus allowing an accurate assessment of I-S.

Cuttings from depths of 1200–2000 m contain mostly dioctahedral phases, which are confirmed by the 060 reflection at 1.499 Å (Figure 5). Dioctahedral smectite in air-dried specimens has a 001 reflection at ~12 Å. After treatment with ethylene glycol, the pattern displays an integral series of higher-order reflections in addition to the first-order reflection at 16.7 Å. Calculated patterns indicate that the smectite has an illite layer content of <20%.

Randomly interstratified (R = 0) I-S with ~45% illite layers also occurs at depths of 2800 and 3000 m. The XRD profile shows that contaminant clay minerals such as kaolinite and discrete illite are present despite the use of the <0.2 μm fraction.

Randomly interstratified I-S is not present in samples below 3400 m; only ordered (R = 1) I-S is present below this depth. Illite layers in the (R = 1) I-S increase with increasing burial depth. A representative pattern of the (R = 1) I-S with 80% illite-layer content shows an intense reflection at 11.1 Å, which is a combination peak of the I-S 002 reflection (24 Å/2 = 12 Å) and the illite 001 reflection (10 Å). After saturation with ethylene glycol, two peaks are resolved at 12.5 and 9.8 Å (Figure 5). The 12.5 Å reflection is a combination of the I-S 002 peak (27 Å /2 = 13.5 Å) and illite 001 peak (10 Å), and the 9.8 Å peak is from the illite 001 and the I-S 003 peaks (27 Å/3 = 9 Å). The sample pattern matches a simulated pattern with 80% illite layers and 20% smectite layers. Layer proportion and ordering type for interstratified I-S are presented in Table 3.

Mineralogy of interstratified chlorite-smectite

Trioctahedral smectite (saponite) is present in samples at depths of 2200–2600 m. The saponite has a first-order basal reflection at ~14.4 Å (Figure 6). Upon saturation with ethylene glycol, a sharp 001 reflection is present at 17.2 Å. An integral series of higher-order reflections is also present in the glycol-treated samples and correlates well with calculated patterns for saponite. The 060 reflection is at 1.537 Å, indicating trioctahedral character.

Corrensite, regularly ordered (1:1) chlorite-smectite (C-S), is present at 3200 m of the SSK-1D well. The corrensite is characterized by a strong superlattice reflection at ~29.2 Å in the air-dried state and the peak shifts to 31.1 Å after glycolation (Figure 6). Other reflections shift from 15.6 to 14.1 Å and from 7.8 to 7.1 Å with ethylene glycol. The superlattice reflection of corrensite is weak in XRD patterns of the <0.2 μm fraction. In the <2 μm fraction, however, the superlattice reflection is strong and sharp and illite, kaolinite

https://doi.org/10.1346/CCMN.2001.0490407 Published online by Cambridge University Press

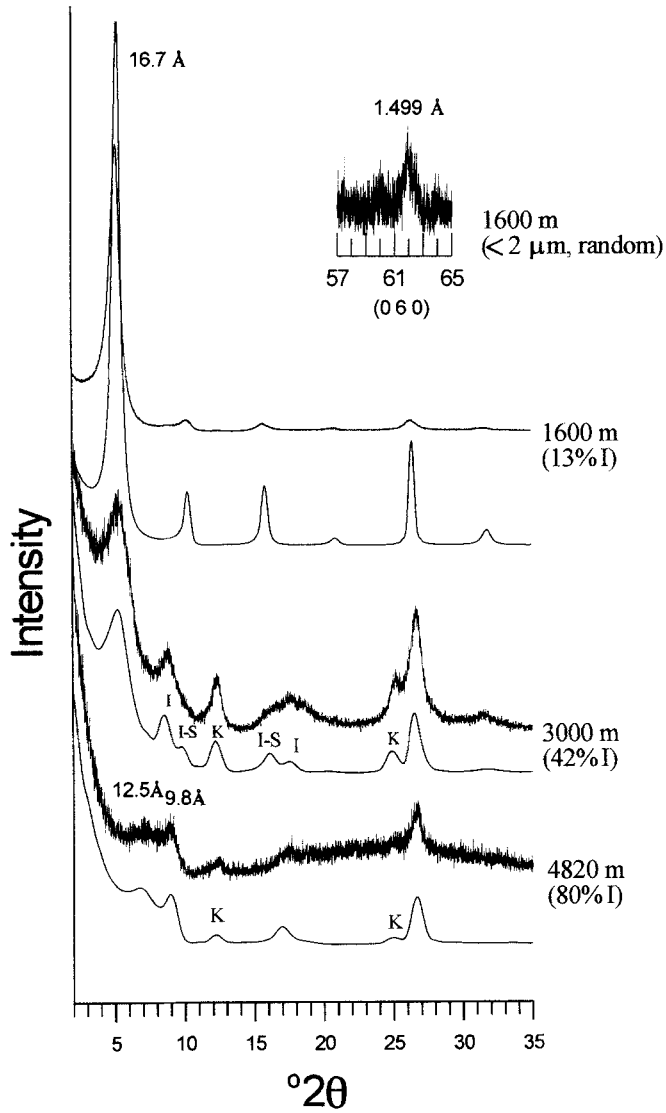

Figure 5. Powder X-ray diffraction patterns of dioctahedral phases. The 060 reflection at 1.499 Å indicates dioctahedral character. I—illite; K—kaolinite; I-S—interstratified illite-smectite.

and quartz are also present in significant amounts. Heating at 550°C produces a peak at ~12 Å. The trioctahedral character of corrensite is shown by the 060 peak position at 1.543 Å.

Chemistry of interstratified illite-smectite

The I-S in seven samples of each <0.2 μm size-fraction sample was analyzed by electron microprobe, and averages are given in Table 4 in order of increasing percentage of illite layers. Samples were analyzed from the shallowest and deepest depths in the well; in the middle depth interval there are no pure samples, even for the <0.2 μm fractions. The chemical analyses of three samples, from 4200, 4400 and 4800 m, were corrected for kaolinite impurities. In addition, the totals were normalized to 100% for comparison (Table 4).

The K and Al contents increase with increasing burial depth, whereas silica content decreases (Figure 7). Illite layers in I-S also increase proportionally with increasing depth of burial. The chemical data are consistent with smectite diagenesis where Al is substituted for Si and interlayer K increases. On average, MgO content increases with depth in shallow intervals, but shows a relative decrease in the deepest samples at ~4800 m. The increase in MgO content at ~1800 m probably reflects the andesitic composition of the rocks present.

Layer charge was plotted (Figure 8) in the triangular diagram of Środoń and Eberl (1984). The data for I-S

https://doi.org/10.1346/CCMN.2001.0490407 Published online by Cambridge University Press

Table 3. Layer proportions of the interstratified clay minerals from the Shinkumoide SK-1D well.

Depth (m)	% I in I-S (<0.2 μm)	Reichweite (R)	% C in C-S	Reichweite (R)
1200	14	R = 0		
1400	20	R = 0		
1600	13	R = 0		
1800	10	R = 0		
2000	20	R = 0		
2200			0	R = 0
2400			0	R = 0
2600			0	R = 0
2800	46			
3000	42			
3200			50	R = 1
3400	65	R = 1		
3600	70	R = 1		
3800	70	R = 1		
4000	75	R = 1		
4200	75	R = 1		
4400	80	R = 1		
4600	80	R = 1		
4800	80	R = 1		
4820	80	R = 1		

at 1200 and 1800 m plot within the range of smectite and random I-S, while those from 4200, 4400 and 4800 m plot within the field of ordered I-S. Thus, the layer-charge data are in good agreement with I-S ratios and ordering types determined by XRD. In this triangular diagram, moreover, the layer-charge data show a notable trend increasing toward higher tetrahedral sheet charge.

Chemistry of trioctahedral smectite

The chemical data for corrensite from 3200 m were not available because contaminant minerals are present in significant amounts in the <0.2 μm fraction. However, samples from 2200 to 2600 m are composed of nearly pure smectite, which was analyzed in detail. Electron-microprobe analyses indicate that the clay fractions from 2200, 2400 and 2600 m consist of smectite (saponite) of trioctahedral nature (Table 5). In general, saponite is characterized by a high Mg content in the octahedral sites. However, saponite from the SSK-1D has a high content of octahedral Al and Fe. In Japan, saponite, C-S and chlorite are common in pyroclastic rocks of the Green Tuff Formations of Miocene age. Saponite occurs in two modes: cavity fillings precipitated from solution and replacement of volcanic glass. Saponite infilling cavities commonly has a high Fe content and low Al content, whereas saponite replacing volcanic glass has high Al and Fe contents (Yoshimura, 1983). According to that author, trioctahedral clay minerals from the Green Tuff Formation have a greater Al content than those from deep-sea basalts. The SSK-1D saponite occurs at middle depths in the well (2200–2700 m) where andesitic pyroclastic rocks are abundant. The SSK-1D saponite is also characterized by high ^{VI}Al and ^{VI}Fe, and is slightly richer in Al than saponites reported from elsewhere in Japan (Figure 9). The Al-rich character suggests that the saponite from the SSK-1D well is derived from fine andesitic volcanic material.

Analyses of the SSK-1D saponite show a low total octahedral occupancy of 5.3–5.5 per 22 oxygens (Table 5), which is well below the ideal value of 6.0. This octahedral vacancy is probably attributable to the oxidation of an originally ferroan saponite. Iron-rich saponite is, in general, unstable under atmospheric conditions when removed from its environment (Badaut *et al.*, 1985). The replacement of OH by O in the octahedral coordination of Fe^{3+} is responsible for the low total octahedral occupancies. Indeed, the original Fe^{2+} content of the SSK-1D saponite can be calculated by multiplying the present Fe^{3+} content by 1.5. This would lead to an increase from $Fe_{1.25}$ to $Fe_{1.88}$ in the formula in Table 5, and thus increases the total octahedral occupancy to 6.0.

DISCUSSION

Alternation of dioctahedral and trioctahedral smectites

In the SSK-1D sequence, we note that dioctahedral and trioctahedral clay mineral phases occur alternately throughout the well (Figure 10). The well provides a rare opportunity to show dioctahedral and trioctahedral clay-mineral diagenesis. In the region including the well, sedimentation and subsidence were relatively uniform throughout their duration without significant deformation, although there are gentle folds and faults caused by compression in the Middle Pleistocene: the sedimentary sequences are deposited conformably in a marine environment during Middle Miocene to Pleistocene time. In addition, there are no hydrothermally intrusive bodies.

The lithology is characterized by the occurrence of fine-grained clastic rocks interbedded with pyroclastic rocks present within the sampled interval. Dioctahedral smectite and trioctahedral smectite (saponite) are present in the upper interval: the dioctahedral smectite at depths of 1000–2000 m dominated by clastics, and the trioctahedral smectite at depths of 2200–2600 m characterized by pyroclastics. Considering the depositional history of the surrounding sediments and the occurrence of the smectite, the SSK-1D smectites have probably altered diagenetically from two parent volcanic materials: dioctahedral smectite at depths of <2000 m is derived from acidic volcanic materials and trioctahedral smectite at 2200–2600 m is derived from basic Mg,Fe-rich volcanic materials. As the depth of burial increases, the dioctahedral smectite reacts to form I-S at 2800–3000 and 3400–4820 m, whereas the trioctahedral smectite converts into a 1:1 regularly interstratified C-S at a depth of 3200 m. Throughout

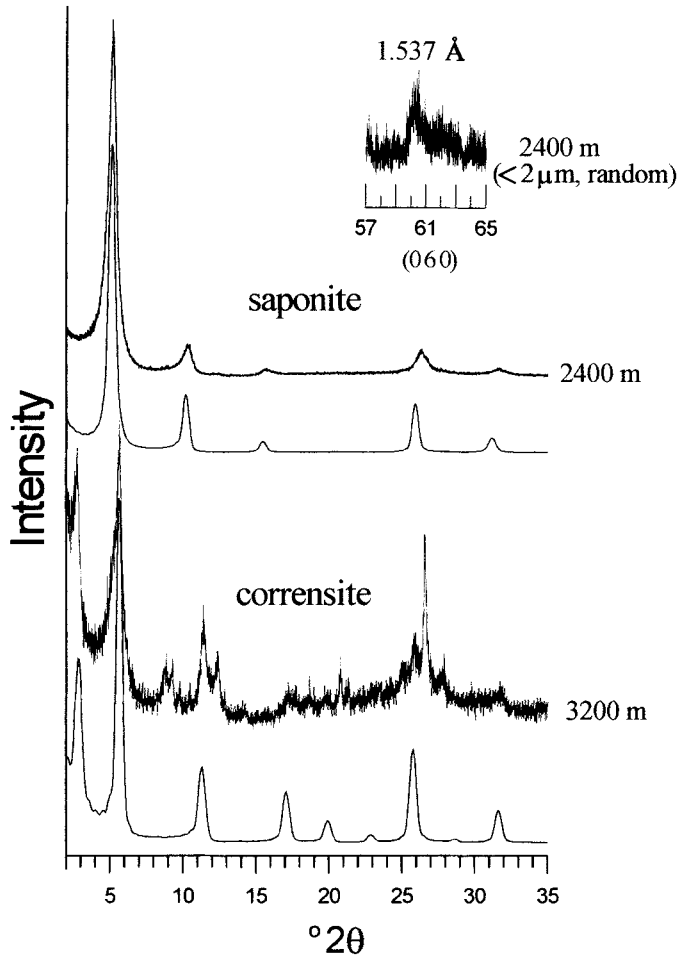

Figure 6. Powder X-ray diffraction patterns of trioctahedral phases. The 060 reflection at 1.537 Å reveals the trioctahedral character.

the interval, as a consequence, I-S and C-S transitions occur alternately: S → I-S → I and S → C-S → C.

Diagenesis of dioctahedral smectite

The I-S transformation is recognized in sedimentary basins worldwide. In the SSK-1D well, the alteration of dioctahedral smectite to I-S conforms to the illitization reaction with an increasing amount of illite layers in response to increasing burial depth. The I-S diagenesis is similar to that of the Gulf Coast (Hower *et al.*, 1976), although trioctahedral smectite and C-S are also present. In the SSK-1D well, the clay mineralogical changes are probably the result of temperature increase associated with burial, because no evidence of igneous or hydrothermal activity was found in the study area.

For the I-S reaction, the pattern of increasing the proportion of illite layers varies among different sedimentary basins worldwide (Środoń and Eberl, 1984). Differences depend primarily on the availability of K, temperature and time. The negative layer charge of the clay becomes sufficiently large to fix K in the interlayers. In the SSK-1D well, the layer charge of I-S increases in the tetrahedral sheet with increasing depth (Figure 8). Moreover, the K and Al contents tend to increase with depth, whereas the Si content decreases (Figure 7), such that: smectite + Al^{3+} + K^{+} → illite + Si^{4+}. In the SSK-1D well, the abundance of K-rich feldspar decreases with depth (Figure 4), thus indicating that K-rich feldspar is the most likely source of K for the I-S reaction. The potassic feldspar is, however, present in trace amounts throughout the well. In addition to the potassic feldspar, therefore, discrete illite, which occurs throughout the well, can be considered as another source of K for the illitization. Futhermore, some I-S may provide the components required to make a more illitic I-S (Pollastro, 1985).

The most striking factor in the I-S reaction is its dependence on temperature. Time is also an important factor in the diagenetic reaction of I-S. In the Gulf

https://doi.org/10.1346/CCMN.2001.0490407 Published online by Cambridge University Press

Table 4. Electron microprobe analysis of interstratified illite-smectite (I-S) from the Shinkumoide SK-1D well.

	Sample depth (% I in I-S)				
	1200 m (14% I)	1800 m (10% I)	4200 m[1] (75% I)	4400 m[1] (80% I)	4800 m[1] (80% I)
SiO_2	62.97	64.10	56.46	56.80	56.33
Al_2O_3	22.73	21.92	26.73	25.84	25.81
Fe_2O_3[2]	7.36	6.83	6.42	6.24	6.91
MgO	2.81	3.42	3.51	3.46	3.30
MnO	0.03	0.06	0.05	0.04	0.02
CaO	0.98	1.07	0.37	0.40	0.57
Na_2O	0.89	1.47	1.05	1.05	0.72
K_2O	2.23	1.12	5.41	6.17	6.34
Total[3]	100.00	100.00	100.00	100.00	100.00
Numbers of cations on the basis of $O_{20}(OH)_4$					
Si	7.61	7.70	7.00	7.06	7.03
Al (IV)	0.39	0.30	1.00	0.94	0.97
Σ tet.	8.00	8.00	8.00	8.00	8.00
Al (VI)	2.85	2.81	2.90	2.85	2.82
Fe	0.67	0.62	0.60	0.58	0.65
Mg	0.51	0.61	0.65	0.64	0.61
Mn	0.00	0.01	0.00	0.00	0.00
Σ oct.	4.03	4.04	4.15	4.08	4.08
Ca	0.13	0.14	0.05	0.05	0.08
Na	0.21	0.34	0.25	0.25	0.17
K	0.34	0.17	0.86	0.98	1.01
Σ int.	0.68	0.65	1.16	1.29	1.26
Tet. chg	0.39	0.30	1.00	0.94	0.97
Oct. chg	0.42	0.49	0.20	0.40	0.36
Int. chg	0.81	0.79	1.21	1.34	1.34

[1] Analysis corrected for kaolinite impurity.
[2] Total Fe as Fe_2O_3.
[3] Total normalized to 100%.

Coast region, for instance, the younger rocks have obviously not changed as much as the old ones, which suggests that the smectite-to-illite reaction is kinetically controlled as a function of time. Based on temperature and geological age, Pollastro (1993) proposed time-temperature models for I-S geothermal studies. The conversion of (R = 0) I-S to (R = 1) I-S is assigned to 100–110°C for sedimentary rocks of Miocene age or older (5–300 Ma) (Hoffman and Hower model; Pollastro, 1993). For younger rocks (<3 Ma), however, the I-S conversion is at a higher temperature of 120–140°C (short-life geothermal model; Pollastro, 1993). In the SSK-1D well, (R = 0) I-S transforms at ~3200 m where corrensite occurs; (R = 1) I-S is found at <3200 m. Therefore, the conversion of (R = 0) I-S to (R = 1) I-S is estimated to occur at a depth of 3200 m. If the Hoffman and Hower model is applied to the conversion, the depth of 3200 m is assigned to 100–110°C. However, if the short-life model is applied, the same depth can be assigned to 120–140°C.

Diagenesis of trioctahedral smectite

In contrast to dioctahedral smectite, trioctahedral smectite (saponite) is converted directly to C-S in the SSK-1D well without any continuous increase in chlorite layers. Some investigators (*e.g.* Chang *et al.*, 1986) interpreted the C-S reaction as a series of interstratified chlorite-smectite phases, analogous to the smectite-to-illite reaction. However, in mafic associations with volcaniclastic sediments, corrensite is considered a discrete mineral, rather than an interstratification of smectite and chlorite layers (Shau *et al.*, 1990; Inoue and Utada, 1991; Beaufort *et al.*, 1997). According to many studies, the S → C-S → C transition does not involve a continuous increase in the number of chlorite layers. Instead, a discrete ratio of smectite and chlorite layers occurs with a discrete stability field. Recently, C-S with >50% chlorite layers was reinterpreted as a physical mixture of corrensite (1:1 C-S) and chlorite (*i.e.* chlorite + corrensite), rather than as interstratified chlorite-smectite (Hillier, 1993).

The SSK-1D saponite is converted to corrensite at a depth of 3200 m. The formation of corrensite from smectite requires the formation of a brucite-like component, and that reaction can be written as: $Mg^{2+} + 2H_2O \rightarrow Mg(OH)_2 + 2H^+$. In the SSK-1D well, saponite is a possible precursor of C-S. Saponite and corrensite occur in the same lithology where andesitic volcaniclastic rocks are predominant. The SSK-1D saponite is an unstable phase, probably because of its high Fe and Al content. Bulk-rock analysis shows that Mg is present in abundance (Table 2) at depths of 2000–2400 m, where saponite exists. Thus, saponite can probably readily transform to more stable corrensite. Consequently, the SSK-1D corrensite is converted diagenetically from saponite by the formation of $Mg(OH)_2$ sheets.

Temperature of smectite diagenesis

Transformation of the clay mineral phases was compared with T_{max} values obtained from organic matter in mudstones by Rock-Eval pyrolysis (Table 6; Figure 10); T_{max} is a pyrolysis temperature where the rate of generation of hydrocarbon is at a maximum during the Rock-Eval pyrolysis reaction (Espitalié *et al.*, 1985). The T_{max} value is a reasonable measure of the thermal maturity of organic matter. Burtner and Warner (1986) found a good correlation between the percentage of smectite layers in I-S and T_{max}. The T_{max} value of 430–435°C, the starting temperature for oil generation, matches well with the conversion of (R = 0) I-S to (R = 1) I-S. In the SSK-1D well, corrensite first occurs at a depth of 3200 m. Moreover, the ordering type of I-S changes at the same depth where corrensite appears, from R = 0 above 3200 m to R = 1 ordering below this depth. The Rock-Eval pyrolysis of organic matter in the SSK-1D mudstones shows a gradual increase in T_{max} value, as shown in Table 6 and Figure 10. Furthermore, a T_{max} temperature of nearly 430–435°C, which is the start of oil generation, occurs to a depth of ~3200 m (Figure 10). The indi-

https://doi.org/10.1346/CCMN.2001.0490407 Published online by Cambridge University Press

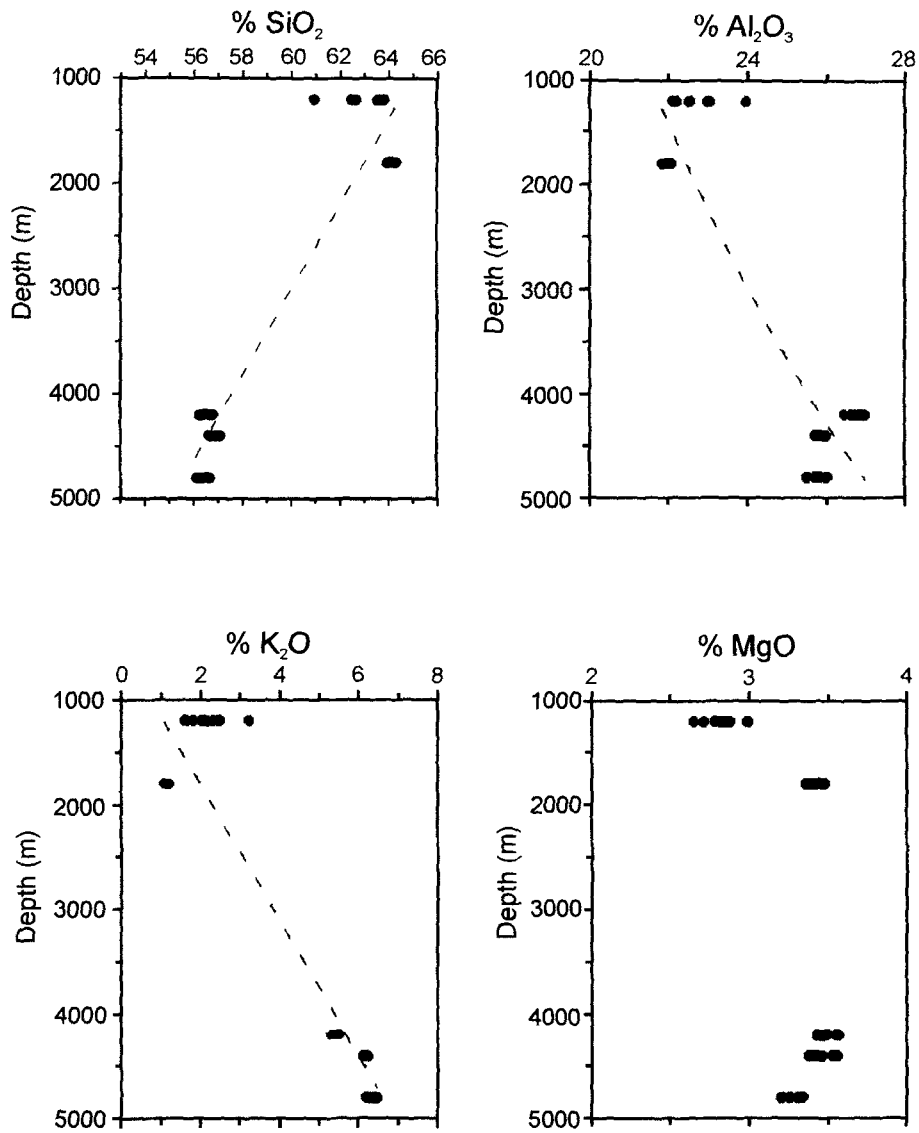

Figure 7. Compositional variation in interstratified I-S with depth.

cators for the degree of diagenesis are consistent: the depth at which (R = 0) I-S is converted to (R = 1) I-S coincides with the depth where corrensite appears and T_{max} of 430–435°C. Thus, the depth of 3200 m is assigned to 100–110°C in accord with the Hoffman and Hower model (Pollastro, 1993). Inoue and Utada (1991) reported that corrensite formed at temperatures of 100–200°C in thermally altered volcaniclastic rocks. This result is consistent with the data here. In addition, Hillier (1993) showed that corrensite occurs at 120–260°C in Devonian lacustrine mudrocks. Iijima and Utada (1971) reported that the formation of corrensite at the expense of trioctahedral smectite was observed at a depth equivalent to 85–95°C which was assigned to the analcime zone. This temperature of first appearance of corrensite was used as a paleothermometer in subsequent studies (Hoffman and Hower, 1979; Pollastro, 1993). Niu *et al.* (2000) studied I-S diagenesis in six wells in the Niigata basin. They showed that there are significant differences between wells at the depth of transition to (R = 1) I-S. The difference may relate either to the influence of other parameters besides temperature, or to uncertainty in the temperatures measured in drill holes, which is neglected in this study. In the Niigata basin, however, a more important factor affecting the difference in the transition of I-S ordering may be tectonic deformation during the Pliocene or Pleistocene. Differences between wells in the depths of transition to the ordering of (R = 1) I-S may be caused by differences in uplift

https://doi.org/10.1346/CCMN.2001.0490407 Published online by Cambridge University Press

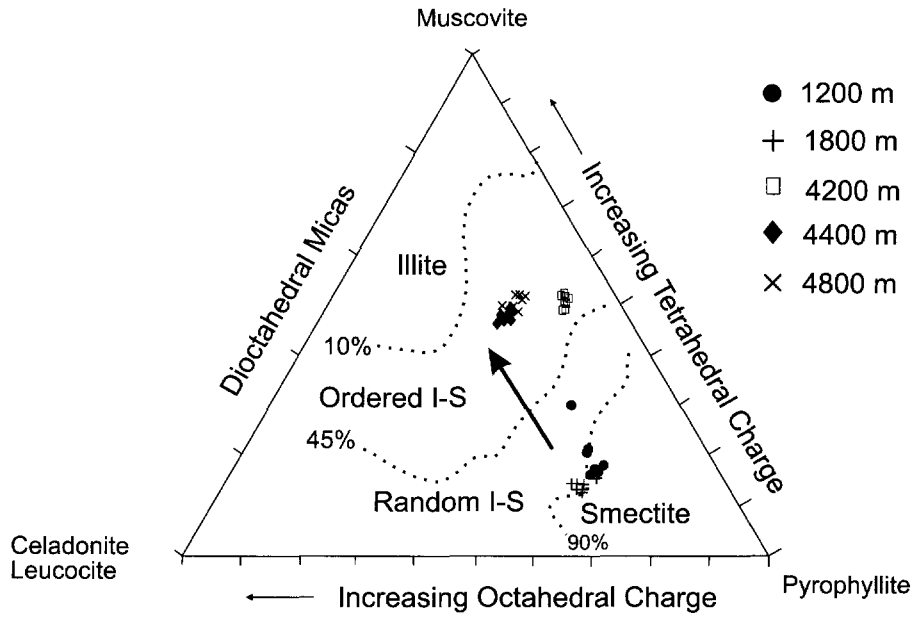

Figure 8. Interstratified I-S plotted within the triangular composition diagram muscovite-celadonite-pyrophyllite (the curves of percent smectite layers are from Środoń and Eberl, 1984). Arrow indicates a trend of increasing tetrahedral layer charge.

and erosion, because burial and tectonic histories vary considerably between areas where the wells are located.

According to temperature data obtained from the Japan Petroleum Exploration Company, the geothermal gradient at the SSK-1D well is 3.10°C/100 m (Figure 11), and the present temperature at 3200 m is 115°C, slightly higher than the temperature of 100–110°C assigned to this depth by the Hoffman and Hower model (Pollastro, 1993). However, the SSK-1D well contains rocks younger than Miocene age in the upper two thirds of the profile. Furthermore, the I-S conversion

Table 5. Electron microprobe analysis of saponites from the Shinkumoide SK-1D and their comparison with other saponites.

	2200 m	2400 m	2600 m	Sudo (1954)	Inoue and Utada (1991)	Niu and Yoshimura (1996)	Kimbara (1975)
SiO_2	50.64	51.69	48.57	39.68	44.18	55.97	40.53
Al_2O_3	12.35	12.49	13.07	3.93	7.86	9.26	12.20
FeO[1]	10.46	10.65	13.77	18.95	15.34	16.20	12.11
MgO	13.35	13.31	12.56	11.21	15.64	14.21	14.44
MnO	0.12	0.11	0.20	0.19	0.08	0.00	0.20
CaO	0.79	0.82	0.47	2.37	2.68	3.65	3.24
Na_2O	1.94	1.23	1.23	0.00	0.00	0.21	0.48
K_2O	0.79	0.81	2.31	0.00	0.30	0.50	1.04
Total	90.44	91.11	92.18	76.33	86.08	100.00	84.24
	Numbers of cations on the basis of $O_{20}(OH)_4$						
Si	7.18	7.25	6.95	7.18	6.87	7.35	6.41
Al (IV)	0.82	0.75	1.05	0.82	1.13	0.65	1.59
Σ tet.	8.00	8.00	8.00	8.00	8.00	8.00	8.00
Al (VI)	1.25	1.31	1.15	0.02	0.31	0.79	0.69
Fe	1.24	1.25	1.65	2.87	1.99	1.78	1.60
Mg	2.82	2.78	2.68	3.02	3.62	2.78	3.41
Mn	0.02	0.01	0.03	0.03	0.01	0.00	0.03
Σ oct.	5.33	5.35	5.51	5.94	5.94	5.35	5.73
Ca	0.12	0.12	0.07	0.46	0.45	0.51	0.55
Na	0.53	0.34	0.34	0.00	0.00	0.05	0.15
K	0.14	0.15	0.42	0.00	0.06	0.08	0.21
Σ int.	0.79	0.61	0.83	0.46	0.51	0.64	0.91

[1] All Fe calculated as FeO.

https://doi.org/10.1346/CCMN.2001.0490407 Published online by Cambridge University Press

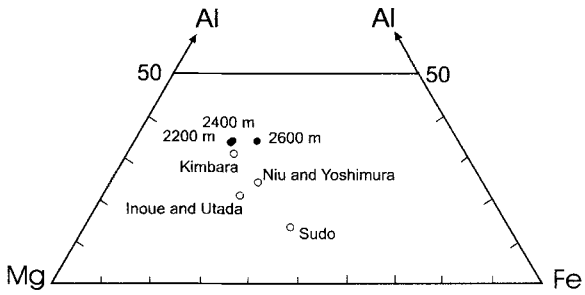

Figure 9. Position of saponite analyses within the triangular composition diagram of Al-Mg-Fe. Data include analyses of saponites from the Shinkumoide SK-1D (solid circle) and other saponites (open circle) from Kimbara (1975), Inoue and Utada (1991), Sudo (1954) and Niu and Yoshimura (1996).

Table 6. Total organic carbon content (TOC) and T_{max} value by Rock-Eval pyrolysis of the mudstones from the Shinkumoide SK-1D well.

Depth (m)	TOC (%)	T_{max} (°C)
1200	0.51	422
1400	0.66	417
1600	0.73	424
1800	0.66	420
2000	0.67	418
2200	0.69	428
2400	0.01	408
2600	0.17	423
2800	0.64	422
3000	0.60	433
3200	0.25	428
3400	0.50	434
3600	0.51	434
3800	0.36	435
4000	0.26	442
4200	0.48	438
4400	0.35	444
4600	0.47	444
4800	0.38	440
4820	0.50	447

also occurs in the Shiiya Formation, mostly deposited during the Pliocene (Figure 2). Therefore, the short-life model can also be applied to the well for estimating paleotemperatures. According to this model, the depth of 3200 m can be assigned to 120–140°C. Assuming that the paleo-geothermal gradient was nearly the same as the present geothermal gradient (Figure 11), the Hoffman and Hower temperature is lower by ~10°C than the present temperature, probably indicating a subsidence of ~ 320 m in depth based on the geothermal gradient. If the short-life model is applicable, the paloeotemperature is greater by ~15°C than the present temperature, thus indicating an uplift of ~500 m. The region incorporating the study well was regionally deformed by an East–West compression during the Middle Pleistocene (~0.7 Ma) (Kobayashi *et al.*, 1991). Considering the effect of the compression, the difference between present and paleotemperatures at a given depth may be caused by uplift or subsidence during the Pleistocene. Uplift, rather than subsidence, is more likely, based on the cross-section (Figure 2). However, a relative subsidence can also occur on the underlying side of a reverse fault, which would be reflected in a paleotemperature lower than the present temperature at greater depths (Son and Yoshimura, 1997). In the SSK-1D well, the interval of the occurrence of corrensite is consistent with that of conversion of (R = 0) I-S to (R = 1) I-S. Therefore, the temperature of formation of corrensite is similar to the temperature of I-S conversion. The profile of SSK-1D includes the geological time of 3–5 Ma, which is not covered by either the Hoffman and Hower model (5–300 Ma) nor the short-life model (<3 Ma). Consequently, the temperature at which corrensite formation commenced in the SSK-1D well is estimated to be 110–120°C, taken from the

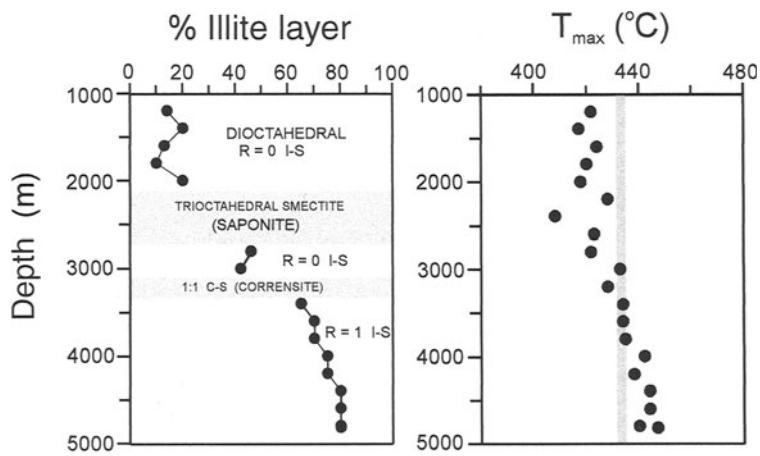

Figure 10. Comparison of variation in clay mineral with T_{max} data by Rock-Eval pyrolysis. Note an alternate occurrence of dioctahedral and trioctahedral phases and an increase in illite layers of I-S.

https://doi.org/10.1346/CCMN.2001.0490407 Published online by Cambridge University Press

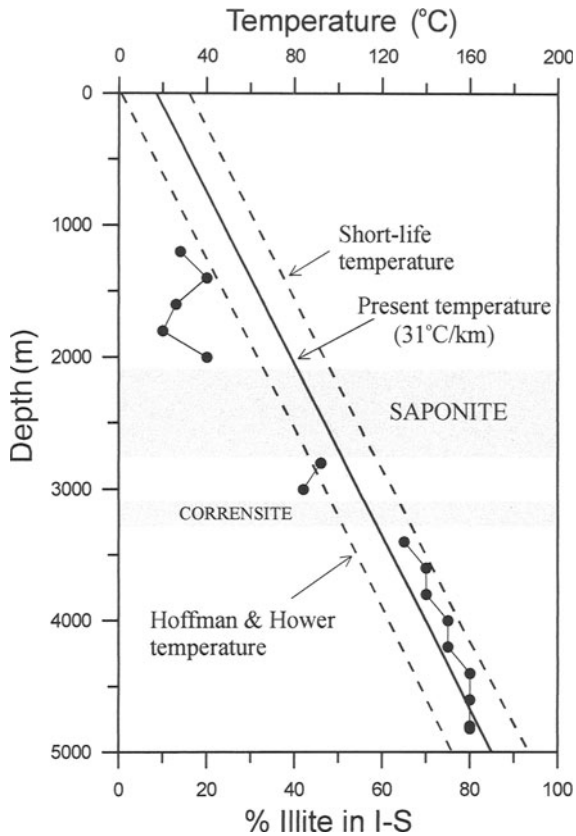

Figure 11. Present-day temperatures and paleo-temperatures deduced from two I-S geothermometry models.

upper temperature of the Hoffman and Hower model and lower value of the short-life model.

ACKNOWLEDGMENTS

The authors are grateful to the Japan Petroleum Exploration Company (JAPEX) for supplying cuttings and granting permission to publish the results. The first author thanks the Japan Society for the Promotion of Science (JSPS) for providing financial support for his study at Niigata University. The manuscript was significantly improved by the comments of S. Guggenheim, D. McCarty, P. Ryan and an unidentified reviewer. This research was supported in part by the NRL program from Korea Ministry of Science and Technology.

REFERENCES

Altaner, S.P. and Ylagan, R.F. (1997) Comparison of structural models of mixed-layer illite/smectite and reaction mechanisms of smectite illitization. *Clays and Clay Minerals,* **45,** 517–533.

Badaut, D., Besson, G., Decarreau, A. and Rautureau, R. (1985) Occurrence of a ferrous, trioctahedral smectite in recent sediments of Atlantis II Deep, Red Sea. *Clay Minerals,* **20,** 389–404.

Beaufort, D., Baronnet, A., Lanson, B. and Meunier, A. (1997) Corrensite: A single phase or a mixed-layer phyllosilicate in the saponite-to-chlorite conversion series? A case study of Sancerre-Couy deep drill hole (France). *American Mineralogist,* **82,** 109–124.

Burtner, R.L. and Warner, M.A. (1986) Relationship between illite/smectite diagenesis and hydrocarbon generation in Lower Cretaceous Mowry and Skull Creek shales of the northern Rocky Mountain area. *Clays and Clay Minerals,* **34,** 390–402.

Chang, H.K., Mackenzie, F.T. and Schoonmaker, J. (1986) Comparisons between the diagenesis of dioctahedral and trioctahedral smectite, Brazilian offshore basins. *Clays and Clay Minerals,* **34,** 407–423.

Elliott, W.C., Aronson, J.L., Matisoff, G. and Gautier, D.L. (1991) Kinetics of the smectite to illite transformation in the Denver basin: Clay mineral, K-Ar data, and mathematical model results. *American Association of Petroleum Geologists Bulletin,* **75,** 436–462.

Eslinger, E. and Pevear, D. (1988) *Clay Minerals for Petroleum Geologists and Engineers.* Society of Economic Paleontologists and Mineralogists, Short Course No. **22,** Tulsa, Oklahoma, 411 pp.

Espitalié, J., Deroo, G. and Marquis, F. (1985) La pyrolyse Rock Eval et ses applications. *Revue de l'Institute Français du Petrole,* **40,** 563–784.

Hillier, S. (1993) Origin, diagenesis, and mineralogy of chlorite minerals in Devonian lacustrine mudrocks, Orcadian basin, Scotland. *Clays and Clay Minerals,* **41,** 240–259.

Hoffman, J. and Hower, J. (1979) Clay mineral assemblages as low grade metamorphic geothermometers: Application to the thrust faulted disturbed belt of Montana. Pp. 55–79 in: *Aspects of Diagenesis* (P.A. Scholle and P.S. Schluger, editors). SEPM Special Publication, **26.**

Hower, J., Eslinger, E.V., Hower, M.E. and Perry, E.A. (1976) Mechanism of burial metamorphism of argillaceous sediment: 1. Mineralogical and chemical evidence. *Geological Society of American Bulletin,* **87,** 725–737.

Iijima, A. and Utada, M. (1971) Present-day zeolitic diagenesis of the Neogene geosynclinal deposits in the Niigata oilfield, Japan. Pp. 342–349 in: *Molecular Sieve Zeolite-I* (R.F. Gould, editor). Advances in Chemistry Series, **101.** American Chemical Society, Washington D.C.

Inoue, A. (1987) Conversion of smectite to chlorite by hydrothermal and diagenetic alterations, Hokuroku kuroko mineralization area, Northeast Japan. Pp. 158–164 in: *Proceedings of the International Clay Conference, Denver 1985* (L.G. Shultz, H. van Olphen and F.A. Mumpton, editors). The Clay Minerals Society, Bloomington, Indiana.

Inoue, A. and Utada, M. (1983) Further investigations of a conversion series of dioctahedral mica/smectites in the Shinzan hydrothermal alteration area, northeast Japan. *Clays and Clay Minerals,* **31,** 401–412.

Inoue, A. and Utada, M. (1991) Smectite-to-chlorite transformation in thermally metamorphosed vocanoclastic rocks in the Kimikita area, northern Honshu, Japan. *American Mineralogist,* **76,** 628–640.

Inoue, A., Kohyama, N., Kitagawa, R. and Watanabe, T. (1987) Chemical and morphological evidence for the conversion of smectite to illite. *Clays and Clay Minerals,* **35,** 115–120.

Kimbara, K. (1975) *Contributions to Clay Mineralogy.* Dedicated to Prof. Toshio Sudo on the occasion of his retirement, Tokyo (in Japanese).

Kobayashi, I. and Yoshimura, T. (2000) *Explanatory text of the Niigata geological map.* Niigata Prefecture, Japan, 199 pp. (in Japanese).

Kobayashi, I., Tateishi, M., Yoshioka, T. and Shimazu, M. (1991) *Geology of the Nagaoka District.* Geological sheet map at 1:50,000, Geological Survey of Japan, Tsuchuba, 132 pp. (in Japanese).

Moore, D.M. and Reynolds, R.C. (1989) *X-ray Diffraction and the Identification and Analysis of Clay Minerals.* Oxford University Press, New York, 332 pp.

Nadeau, P.H., Wilson, M.J., McHardy, W.J. and Tait, J.M. (1984) Interparticle diffraction: A new concept for interstratified clays. *Clay Minerals,* **19,** 757–769.

Niu, B. and Yoshimura, T. (1996) Smectite conversion in diagenesis and low grade hydrothermal alteration from Neogene basaltic marine sediments in Niigata Basin, Japan. *Clay Science,* **10,** 37–56.

Niu, B., Yoshimura, T. and Hirai, A. (2000) Smectite diagenesis in Neogene marine sandstone and mudstone of the Niigata basin, Japan. *Clays and Clay Minerals,* **48,** 26–42.

Perry, E.A. and Hower, J. (1972) Late-stage dehydration in deeply buried pelitic sediments. *American Association of Petroleum Geologists Bulletin,* **56,** 2013–2021.

Pollastro, R.M. (1985) Mineralogical and morphological evidence for the formation of illite at the expense of illite/smectite. *Clays and Clay Minerals,* **33,** 265–274.

Pollastro, R.M. (1993) Considerations and applications of the illite/smectite geothermometer in hydrocarbon-bearing rocks of Miocene to Mississippian age. *Clays and Clay Minerals,* **41,** 119–133.

Pytte, A.M. and Reynolds, R.C. (1989) The thermal transformation of smectite to illite. Pp. 133–140 in: *Thermal History of Sedimentary Basins* (N.D. Naeser and T.H. McCulloh, editors). Springer-Verlag, New York.

Reynolds, R.C. Jr. (1985) *NEWMOD: A computer program for the calculation of the one-dimensional patterns of mixed-layered clays.* R.C. Reynolds, 8 Brook Rd., Hanover, New Hampshire.

Sato, T., Kudo, T. and Kameo, K. (1995) On the distribution of source rocks in the Niigata oil field based on the microfossil biostratigraphy. *Journal of the Japanese Association for Petroleum Technology,* **60,** 76–86 (in Japanese).

Shau, Y.-H., Peacor, D.R. and Essene, E.J. (1990) Corrensite and mixed-layer chlorite/corrensite in metabasalt from northern Taiwan: TEM/AEM, EPMA, XRD, and optical studies. *Contributions to Mineralogy and Petrology,* **105,** 123–142.

Sietronics (1996) *SIROQUANT: A quantitative XRD software.* Sietronics Pty Limited, Belconnen ACT, Australia.

Son, B.-K. and Yoshimura, T. (1997) The smectite-to-illite transition in the Koyoshigawaoki well in the Akita sedimentary basin, Northeast Japan. *Clay Science,* **10,** 163–183.

Środoń, J. and Eberl, D.D. (1984) Illite. Pp. 495–544 in: *Micas* (S.W. Bailey, editor). Reviews in Mineralogy, **13.** Mineralogical Sciety of America, Washington, D.C.

Sudo, T. (1954) Iron-rich saponite found from Tertiary iron sand beds of Japan. *Journal of Geological Society of Japan,* **60,** 18–27.

Yoshimura, T. (1983) Neoformation and transformation of trioctahedral clay minerals in diagenetic process. *Journal of Sedimentology of Japan,* **17–19,** 177–185 (in Japanese).

E-mail of corresponding author: sbk@rock25t.kigam.re.kr
(*Received 11 May 2000; revised 22 February 2001; Ms. 448; A.E. Douglas K. McCarty*)